12.4   HIGH RESOLUTION ANALYSES OF THE 8 MAY 2003 OKLAHOMA CITY STORM,
PART I: STORM STRUCTURE AND EVOLUTION FROM RADAR DATA

Donald W. Burgess

Cooperative Institute for Mesoscale Meteorological Studies, University of Oklahoma, Norman, OK

1.   INTRODUCTION

The use of radar to diagnose thunderstorm structure and evolution has been going on since the birth of weather radar during and just after World War II. In particular, studies of supercell storms have been most insightful (Browning 1964).   Insights about useful structures within radar reflectivity and velocity data fields have led to better understanding of storm dynamics, operational applications, and improvements in severe storm and tornado warnings.

The current research effort is designed to determine the structure and evolution of one storm (the Oklahoma City tornadic supercell of 8 May 2003) from as many radars and with as much detail as possible (Part I), assimilate the observations and numerically model the storm (Part II; Dowell et al. 2004), and perform ultra-high resolution model experiments of tornadogenesis (Part III; Wicker and Dowell 2004). This paper reports on the structure and evolution of the Oklahoma City storm as seen by data from the central Oklahoma WSR-88D (KTLX), and analyzed through use of the NSSL WDSSII system (Hondl 2003). The storm formed ~110 km southwest of KTLX and moved to within 20 km during its tornadic phase, meaning that the radar beamwidth was always less than 2 km, mostly less than 1 km, and the radar horizon was at cloud base or below for much of the storm's life. With such data in 5-minute volumes, the overall structure and evolution of the storm can be studied. KTLX is not polarized, but polarization information is available from another central Oklahoma radar (KOUN). Only small amounts of KOUN data are a part of this analysis, but more detailed analyses of KOUN data are underway and will be reported later.

2.   STRUCTURE AND EVOLUTION

The Oklahoma City storm began at ~2040 (all times are UTC) as part of a cluster of several small convective cells that formed along and just east of a dryline in west-central Oklahoma (Fig. 1a). As other small cells dissipated, the Oklahoma City storm grew, in

part because of mergers with cells that formed to the rear and along the right flank of the storm. The merged storm obtained classic supercell characteristics (hook echo and Bounded Weak Echo Region (BWER); Fig. 1b).   Also, two classic left splits occurred during the storm's maturing phase. The storm produced a weak (F0) and very short-lived (<1 minute) tornado at 2200. A second weak (F0) tornado occurred from 2204 to 2208, momentarily dissipating, only to redevelop as a violent (F4) long-lived tornado at 2210.   The third tornado tore a 27-km path through Moore (F2) and southeast Oklahoma City (F4), dissipating at 2238. During its most intense/damaging period, the tornado lofted large amounts of debris, producing a very highly reflective "knob" within the tip of the hook (Fig. 1c; see Burgess et al. 2002 for a similar debris signature associated with a 3 May 1999 tornado).

During the latter portion of the F4 tornado life time, the storm mesocyclone underwent an occlusion (Burgess et al. 1982) with the tornadic circulation center turning leftward to be within the storm core and a new circulation center and hook echo forming along the right-flank gust front.   The new circulation center continued the supercell phase, but neither it nor an even later circulation center was as strong as the tornadic circulation, and no additional tornadoes were reported. The storm completely dissipated by ~0000 on 9 May.

A time/height diagram of the maximum reflectivity at each elevation angle (Fig. 2a) provides more detail about storm evolution. After a very short-lived first cell (~2040), a large, strong, tall cell developed by 2100 and briefly produced 65 dBZ aloft. The initial strong cell weakened and was replaced by a new rear cell (2121; 1st Fig. 2 upward pointing arrow) that quickly strengthened. As indicated by the 2nd and 3rd upward pointing arrows (Fig. 2), right-flank cells merged into the storm at 2141 and 2151. After the mergers, the storm grew very strong with a 70-dBZ core that extended to heights greater than 10 km above radar level. During the time period of the F4 tornado and the mesocyclone occlusion, the strong core descended toward the surface, presumably because of weakening updraft. After 2230, no elevated, highly reflective core was detected, although a large area of 60 DBZ reflectivity continued.

A companion time/height diagram of maximum azimuthal shear or azimuthal vorticity (the component of vertical vorticity sensed by a single-Doppler radar) at each elevation angle (Fig. 2b) provides more detail

Corresponding author address: Don Burgess, Cooperative Institute for Mesoscale Meteorological Studies, 1313 Halley Circle, Norman, OK, 73069; Donald.Burgess@noaa.gov
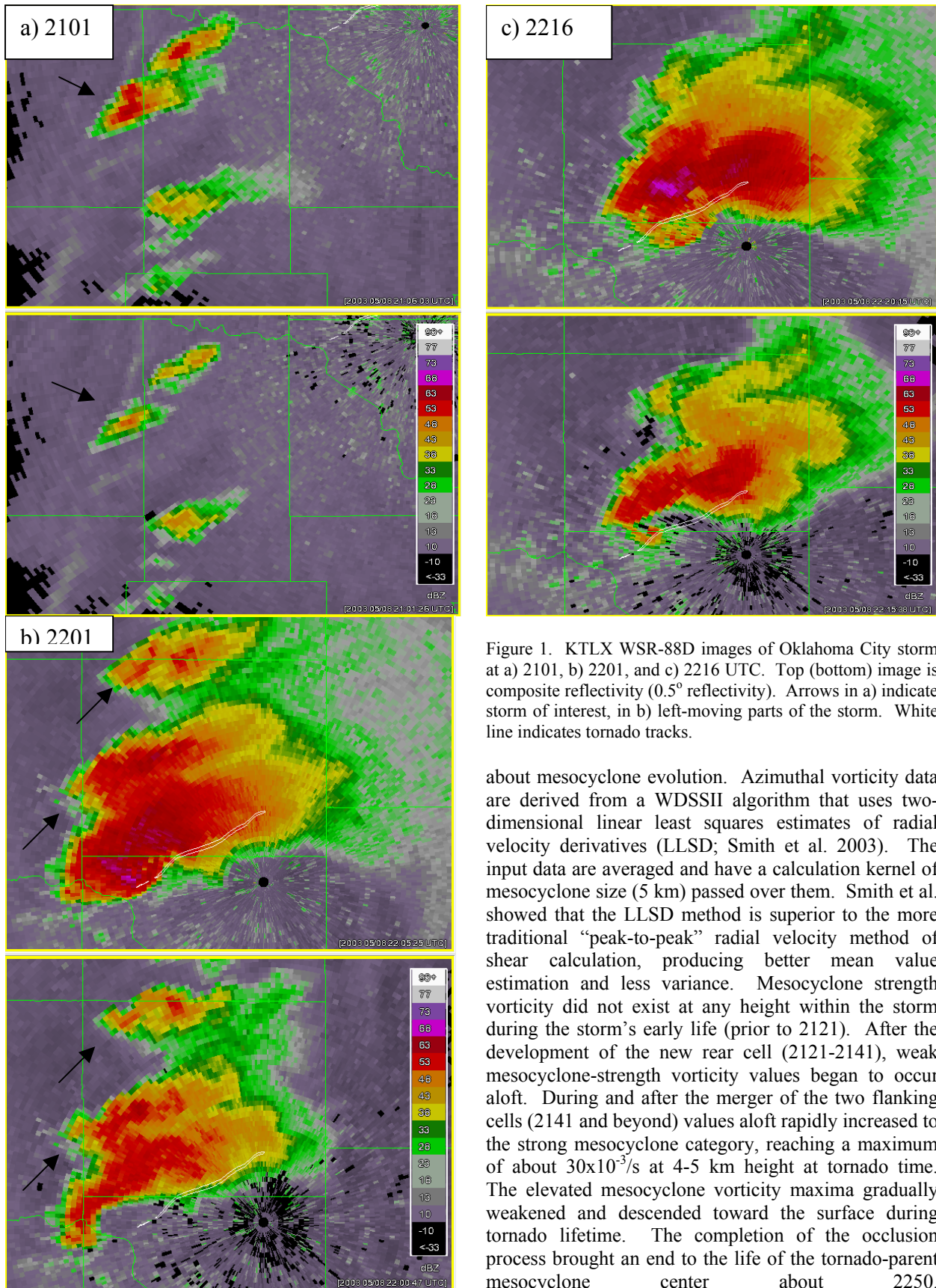
Figure 1. KTLX WSR-88D images of Oklahoma City storm at a) 2101, b) 2201, and c) 2216 UTC. Top (bottom) image is composite reflectivity (0.5^o reflectivity). Arrows in a) indicate storm of interest, in b) left-moving parts of the storm. White line indicates tornado tracks.

about mesocyclone evolution. Azimuthal vorticity data are derived from a WDSSII algorithm that uses two-dimensional linear least squares estimates of radial velocity derivatives (LLSD; Smith et al. 2003). The input data are averaged and have a calculation kernel of mesocyclone size (5 km) passed over them. Smith et al. showed that the LLSD method is superior to the more traditional "peak-to-peak" radial velocity method of shear calculation, producing better mean value estimation and less variance. Mesocyclone strength vorticity did not exist at any height within the storm during the storm's early life (prior to 2121). After the development of the new rear cell (2121-2141), weak mesocyclone-strength vorticity values began to occur aloft. During and after the merger of the two flanking cells (2141 and beyond) values aloft rapidly increased to the strong mesocyclone category, reaching a maximum of about 30x10^{-3}/s at 4-5 km height at tornado time. The elevated mesocyclone vorticity maxima gradually weakened and descended toward the surface during tornado lifetime. The completion of the occlusion process brought an end to the life of the tornado-parent mesocyclone center about 2250.
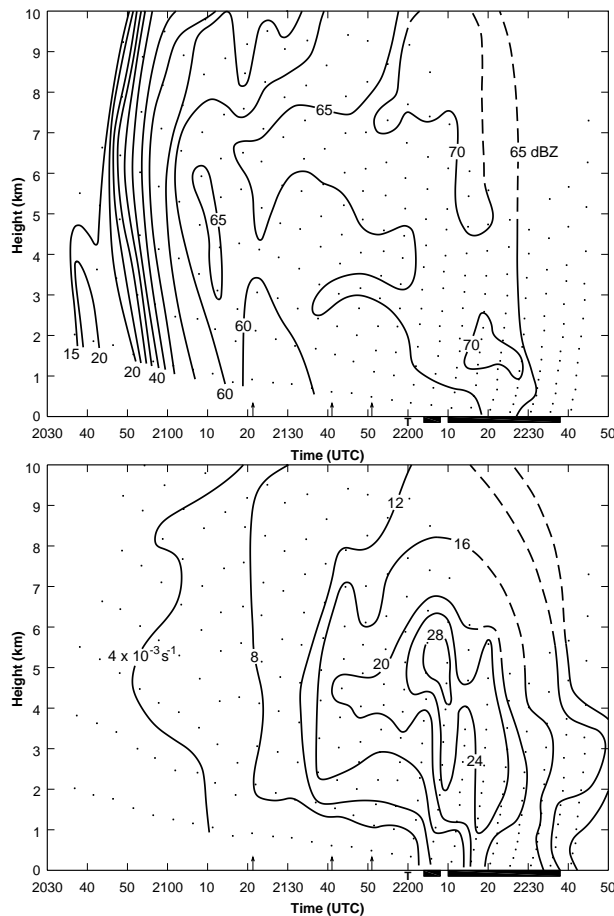
Figure 2. Time/height diagrams of a) reflectivity (top) and b) azimuthal vorticity (bottom). Dots are individual data points. Up pointing arrows along x-axis mark cell changes. T and dark bars along x-axis indicate tornado times.

As has been seen with a number of supercells (Burgess and Magsig 1993 and 1998), the low-level mesocyclone was slower to develop. Near cloud base and below, mesocyclone strength vorticity did not appear until tornado time (2200), but did increase rapidly after that time, reaching a maximum of about 20×10^{-3}/s.

3. DISCUSSION

Studies of supercell storms usually strive to identify and explain the interrelationship between two quantities, updraft strength and vertical vorticity strength. Using only single Doppler radar, these are challenging entities to quantify since neither is directly or completely measured. A number of parameters derived from reflectivity data have been chosen to indirectly infer changes in storm updraft strength: height of max reflectivity, Severe Hail Index (SHI), BWER existence and top height, and Zdr column height. SHI (Witt et al. 1998) is a vertical integration of reflectivity values above the freezing level (~4.2 km on 8 May) and

is related to updraft strength as well as severe hail. The KTLX radar has not as yet been polarized so data from the NSSL long-term test-bed radar (KOUN) have been added[*]. Zdr columns are thought to arise from liquid water drops created and elevated in strong updrafts. When all the reflectivity parameters are graphed (Fig. 3), a somewhat confusing pattern results. However, a blending of all values suggests that there were three peaks in updraft strength: one with the early cell (before 2121), one with the rear cell (2121-2141), and one with the merged cells (>2141). The latter peak (>2141) appeared to be the strongest updraft time period with a BWER and the highest values for the other parameters. The Fig. 3 analysis does not continue after 2201 because of the close approach of the storm to KTLX and KOUN. Cone-of-silence problems (see Fig. 2 for a distribution of data points) prevented meaningful parameter estimates after 2201.

Azimuthal shear/vorticity (and assumed circular flow symmetry within the mesocyclone) is used as a proxy to infer changes in vertical vorticity (Fig. 4). Only weak vorticity was present with the first cell (<2121). Mid-level mesocyclone vorticity (as depicted by the 4.5 km value) increased during the time period of the rear cell (2121-2141), and was at a maximum during the merged cells (~2200). In contrast, low-level mesocyclone vorticity (as depicted by the 1 km value) was weak until tornado time (~2200) when there was a rapid increase. Note that after 2216 low-level vorticity values were higher than mid-level values. During this period (also the time period of occlusion), the stronger low-level rotation (and assumed lowest pressure) may have resulted in a downward directed pressure gradient force within the mesocyclone that reduced updraft magnitude. A closer look at the low-level mesocyclone can be obtained by examining data during the interval when most of the KTLX radar beam energy was below cloud base (~ 1 km cloud base height from the 00 UTC OUN sounding). Figure 5 is a graph of the 0.5 km azimuthal vorticity and 0.5 km radial convergence at 2146 and after. In agreement with similar past studies (Burgess and Magsig 1993 and 1998), a significant increase in low-level convergence precedes the rapid increase in low-level vorticity and tornadogenesis. The time of the very strong low-level convergence (~2200) coincides with the time of the strongest updrafts inferred from the reflectivity parameters. Radial convergence values after 2216 are not shown because the measured values at later times appeared more related to the development of the new circulation center along the gust front than the older, occluding circulation.

---

[*] Zdr columns are being analyzed in a concurrent 2004 REU summer student project.
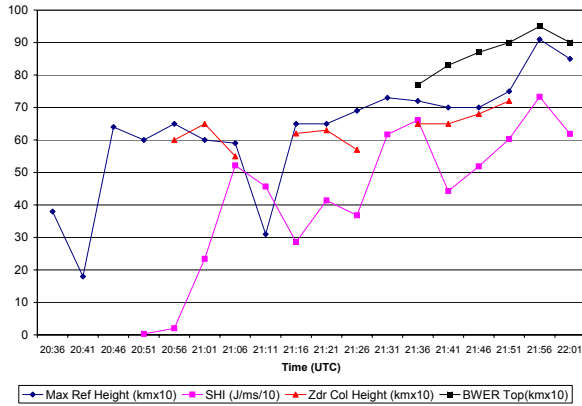
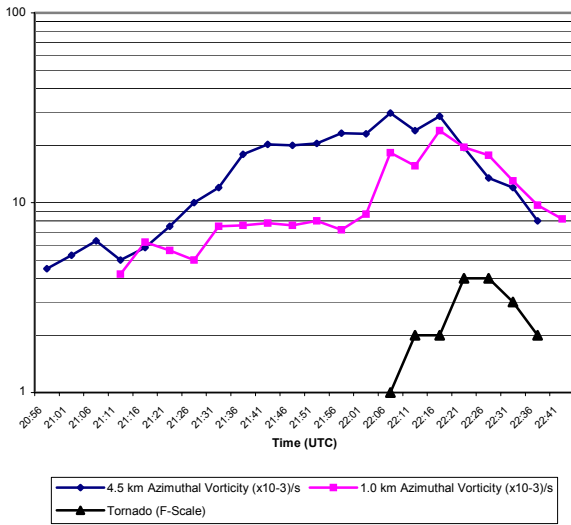Figure 3. Graph of reflectivity parameters.

Figure 4. Graph of mid-level (4.5 km), low-level (1.0 km) azimuthal vorticity, and tornado F-Scale.

4. CONCLUSIONS AND FUTURE WORK

Analysis to this point has emphasized the overall storm and mesocyclone scales within the storm, concentrating on data from the KTLX radar. The May 8th supercell was composed of three phases: a moderately strong early cell that did not possess much rotation, a stronger rear-forming cell with a developing mid-level mesocyclone, and a post-merger of cells storm that was very strong, producing intense updraft, intense rotation, and tornadoes. The sequence of new cell development and cell merger to arrive at the very strong phase is a somewhat unique characteristic of this storm. However, the characteristics of the resulting mature storm are similar to a number of past studies; strong rotation aloft, weak rotation but strong convergence at cloud base,
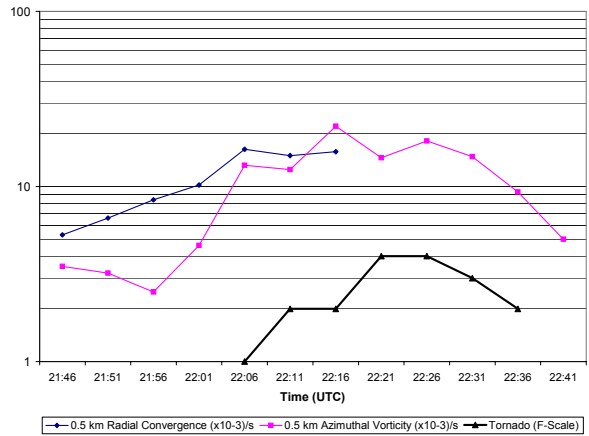

Figure 5. Graph of 0.5 km radial convergence, 0.5 km azimuthal vorticity, and tornado F-scale.

followed by rapid increase in low-level rotation and concomitant tornadogenesis.

Future study will focus in three areas: 1) gaining a better understanding of storm updraft evolution and microphysics, 2) gaining a better understanding of the small-scale structure and evolution of vorticity and associated tornadogenesis, and 3) comparison of all observed characteristics to the on-going numerical model portion of the study. The 8 May KOUN data provide exciting opportunity for study of polarization information related to supercell evolution and tornadogenesis (see Schurr et al. 2004 for information on the 8 May polarization tornado debris signature). The 8 May OKC-area TDWR data provide exciting opportunity for high-resolution study of time and space scales not sampled by KTLX or KOUN. A side benefit might be better understanding of TVS signatures (seen by KTLX and KOUN, but as yet not examined). Finally, all storm observations (including microphysical information) can be compared to the storm-scale and tornado-scale simulations of the 8 May storm that are now being developed. The completeness of the model vertical velocity and vorticity fields will provide new insights into limitations associated with the remote sensors (radars).

5. ACKNOWLEDGMENTS

6. REFERENCES

Browning, K.A., 1964: Airflow and precipitation trajectories within severe local storms which travel to the right of the winds. *J. Atmos. Sci.*, **21**, 634-639.

Burgess, D.W., and M.A. Magsig, 1993: Evolution of the Red Rock, Oklahoma supercell of April 26,1991. Preprints, *17th Conf. Severe Local Storms*, St. Louis, MO, AMS, 257-261.

_____,_____, 1998: Recent observations of tornado development at near range to WSR-88D radars. Preprints, *19th Conf. Severe Local Storms*, Minneapolis, MN, AMS, 756-759.

_____, V.T. Wood, and R.A. Brown,1982: Mesocyclone evolution statistics. Preprints, *12th Conf. Severe Local Storms*, San Antonio, TX, AMS, 84-89.

_____, M.A. Magsig, J. Wurman, D.C. Dowell, and Y. Richardson, 2002: Radar observations of the 3 May 1999 Oklahoma City tornado. *Wea. and Forecasting*, **17**, 456-471.

Dowell, D.C., L.J. Wicker, and D.J. Stensrud, 2004: High resolution analysis of the 8 May 2003 Oklahoma City storm. Part II: EnKF data assimilation and forecast experiments. Preprints, *22nd Conf. Severe Local Storms*, Hyannis, MA, AMS, this volume.

Hondl, K.D., 2003: Capabilities and components of the Warning Decision Support System-Integrated Information (WDSSII). Preprints, *19th Intnl. Conf. on Interactive Information and Processing Systems (IIPS)*, Long Beach, CA, AMS, CD preprint #14.7.

Schurr, T.J., A.V. Ryzhkov, D.W. Burgess, and D.S. Zrnic, 2004: Polarimetric radar observations of tornadic debris signatures. Preprints, *22nd Conf. Severe Local Storms*, Hyannis, MA, AMS, this volume.

Smith, T.M., K.L. Elmore, G.J. Stumpf, and V. Lakshmanan, 2003: Detection of rotation and boundaries using two-dimensional, local, linear least squares estimates of velocity derivatives. Preprints, *31st Conf. Radar Meteor.*, Seattle, WA, AMS, 310-313.

Wicker, L.J., and D.C. Dowell, 2004: High resolution analysis of the 8 May 2003 Oklahoma City storm. Part III: An ultra-high resolution forecast experiment. Preprints, *22nd Conf. Severe Local Storms*, Hyannis, MA, AMS, this volume.

Witt, A., M.D. Eilts, G.J. Stumpf, J.T. Johnson, E.D. Mitchell, and K.W. Thomas, 1998: An enhanced hail detection algorithm for the WSR-88D. *Wea. and Forecasting*, **13**, 286-303.